

# <sup>1</sup>Long-Distance Signal Propagation in AC-LGAD

C. Bishop, A. Das, J. Ding, M. Gignac, F. Martinez-McKinney, S. M. Mazza, A. Molnar,  
N. Nagel, M. Nizam, J. Ott, H. F.-W. Sadrozinski, B. Schumm, A. Seiden, T. Shin,  
A. Summerell, M. Wilder, Y. Zhao

*SCIPP, Univ. of California Santa Cruz, CA 95064, USA*

*Abstract*– We investigate the signal propagation in AC-LGAD (aka RSD), which are LGAD with a common  $N^+$  layer and segmented AC-coupled readout contacts, by measuring response to IR laser TCT on a large selection of AC-LGAD with strip readout. The interest for this topic derives from the realization that while large charge sharing between neighboring strips is essential for good position resolution, large sharing beyond the next neighbor generates background signals which in general are detrimental to the sensor goal of low occupancy. Using AC-LGAD with strip readout produced by Hamamatsu Photonics (HPK), we evaluate the effects of a variety of sensor properties, including geometrical parameters (strip length, width), process parameters like the  $N^+$  layer resistivity, the coupling capacitance, and the thickness of the bulk on the signal sharing and the position resolution.

PACS: 29.40.Gx, 29.40.Wk, 78.47jc

Keywords: fast silicon sensors; charge multiplication; AC-LGAD strips; charge sharing.

## 1. Introduction

Low-gain Avalanche Detectors (LGAD) have been recently introduced as fast semiconductor timing sensors [1,2]. In their experimental applications their segmentation is limited to pads with 1 mm pitch by consideration of power and fill-factor. To avoid this restriction which limits the spatial resolution, the AC-LGAD technology (aka Resistive Silicon Detector RSD) [3-5] is under investigation, based on a complete integration of four of the sensor layers in common sheets of the P-type bulk, the  $P^+$  gain layer, the  $N^+$  layer and a dielectric sheet, separating the first three from the segmented metal readout contacts (Fig. 1). A signal originating in the bulk and amplified in the gain layer is then shared between several electronics channels, allowing reconstruction of signal location with a resolution which is a small fraction of the readout pitch. Yet due to the common  $N^+$  layer, the observed signal in AC-LGADs is the sum of the directly induced signal from the moving collected charge on neighboring contacts (shown in red in Fig. 1) and the pick-up of the signal conducted on the  $N^+$  layer common to all contacts (“leakage” shown in yellow).

The relative strength between induced and conducted signal depends on a variety of sensor parameters which we compare in the following study using scanning laser Transient Current Technique (TCT) on strip AC-LGAD produced by HPK : the geometry of the metal readout contacts was varied, as were production details of two common layers ( $N^+$  layer resistivity and dielectric specs) and the bulk thickness. The doping

of the gain layer and the strip pitch were kept constant. This will allow to check the simple assumption that for a large local signal and a small amount of long-distance conducted signal a large  $N^+$  resistivity and a large coupling capacitance are needed.

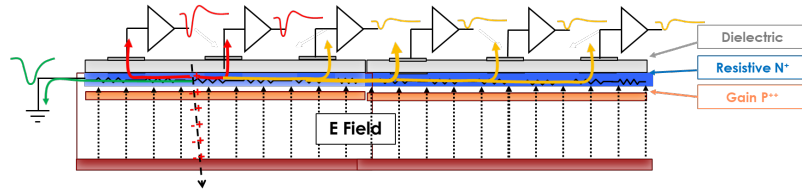


Fig. 1 Cross section of an AC-LGAD showing common sensor layers and the signal shared by neighboring metal contacts.

## 2. Experimental

### 2.1 Sensors

The sensors used were fabricated by HPK as part of the US-Japan Collaborative Agreement [6]. Two values for the  $N^+$  sheet resistance and two values for the capacitance of the coupling capacitance were selected, resulting in four basic sensor types as shown in Fig. 2 LEFT.

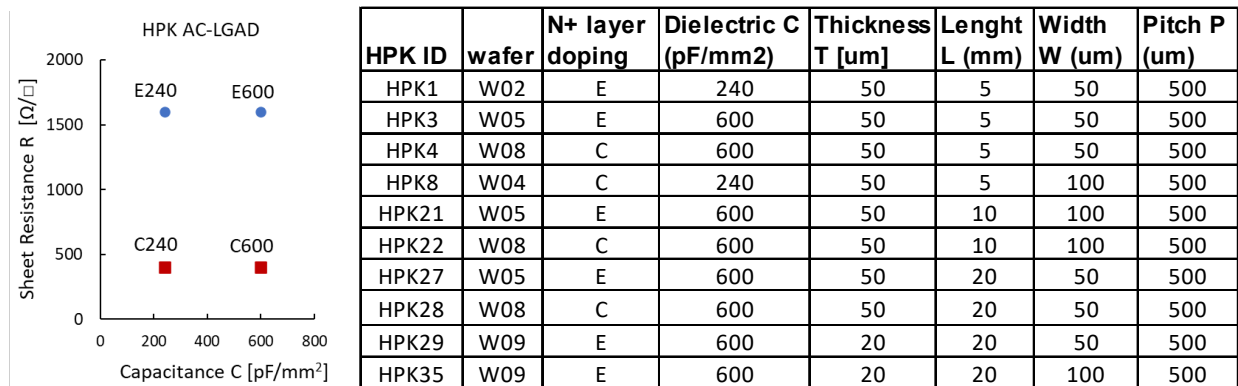


Fig. 2 LEFT: Selected values for the sheet resistance of the  $N^+$  layer and for the capacitance per area of the coupling capacitance. RIGHT: Parameters for the HPK AC-LGAD tested

The detailed sensor layout was then achieved by selecting two thicknesses of the bulk (50 and 20  $\mu\text{m}$ ), and for the metal strips, two widths (50 and 100  $\mu\text{m}$ ), and three length (5, 10, 20 mm) on a 500  $\mu\text{m}$  pitch as shown in Fig. 2 RIGHT. This way all four of the selection in Fig. 2 are realized and could be compared. It should be pointed out that the actual value of the coupling capacitance varies between 60 pF and 1200 pF.

### 2.2 IR Laser TCT Measurements

The charge collection measurements using TCT follow the method described in [7]. In short, the sensors are mounted on fast analog amplifier boards with 16 channels and 1 GHz of bandwidth designed at Fermilab (FNAL) [8] and read out by a fast oscilloscope (2 GHz, 20 Gs). Sensors mounted on boards are excited with an infrared (IR) 1064 nm pulsed laser with a pulse temporal width of 400 ps, and a spot of 10-20  $\mu\text{m}$

width mimicking the response of a MIP in the silicon [9]. The IR laser cannot penetrate the metal strips, therefore the sensor behavior can be characterized only in between metal electrodes.

The read-out board is mounted on X-Y moving stages so the response of the sensor as a function of laser illumination position can be evaluated. Waveforms are averaged to decrease the effect of laser power fluctuations, and a photodiode is used to correct for them. The scans were analyzed using the pulse shape in each position to derive pulse maximum (Pmax) [7]. In addition, the rise time and fall time and the time of arrival were recorded and will be the topic of a later publication.

### 3. Results and Discussion

#### 3.1 Pulse Height Pmax

An important parameter of the LGAD is the internal gain, which multiplies the generated pulse charge to the level of the collected charge. Yet most of the LGAD investigations of timing or location precision involve the pulse height instead of the charge. The maximum pulse height, Pmax, depends on the bias voltage as shown in Fig. 3. The bias voltages shown values are below the on-set of breakdown. The logarithmic presentation shows the exponential gain dependence to be similar for all sensors, but the data separate along being E-type (purple) or C-type (reddish). Sensors with longer strips require larger bias voltage to reach the same Pmax. Sensors with bulk thickness  $T = 20 \mu\text{m}$  and  $T = 50 \mu\text{m}$  show essentially the same Pmax range due to different weight fields and rise times. At a noise value of  $2 \text{ mV}$ ,  $S/N = 100$  for  $P_{\text{max}} = 200 \text{ mV}$ .

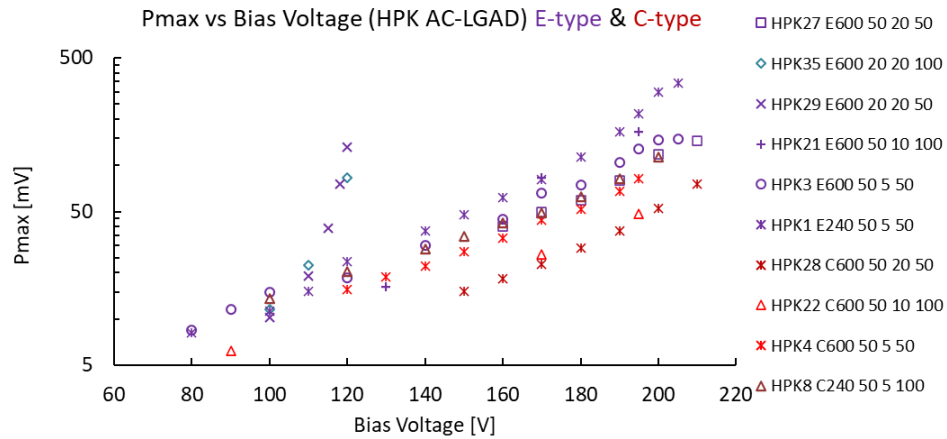


Fig. 3 Bias voltage dependence of the pulse height Pmax for the tested AC-LGADs (Legends : ID#, Type, Thickness T, Strip Length L, Strip Width W)

#### 3.2 Pulse Sharing

The pulse sharing is tested in positional laser (TCT) scans with normalized Pmax as shown in Fig.4, with Fig. 4 LEFT representing the 4 different combinations of  $N^+$  sheet resistance R and dielectric capacitance C indicated in Fig. 2. They all have a length  $L = 5 \text{ mm}$  and thickness  $T = 50 \mu\text{m}$ , and metal width  $W = 50 \mu\text{m}$ , except for C240, which has  $W = 100 \mu\text{m}$ . (N.B.: most of the positional scans exhibit increases at the two ends, being attributed to the pick-up from the  $N^+$  layer contact). Different sensors show different signal sharing properties according to the Type used:

- E600 and E240 (high R) have optimal close signal sharing contained within the strip center of the next neighbor, getting reduced to 2 – 3 % “leakage” at long distance, with E600 preferred;
- C600 (low R, high Cap) has large sharing close to and beyond next neighbor, exhibiting long-distance constant “leakage” of the order of 10%;
- C240 (low R, low Cap) has large sharing to the next few neighbors, with the long-distance “leakage” reduced to < 2%.

This large sharing in the C-Type sensors appears to be the root cause for the reduced Pmax compared to E-types shown in Fig. 3.

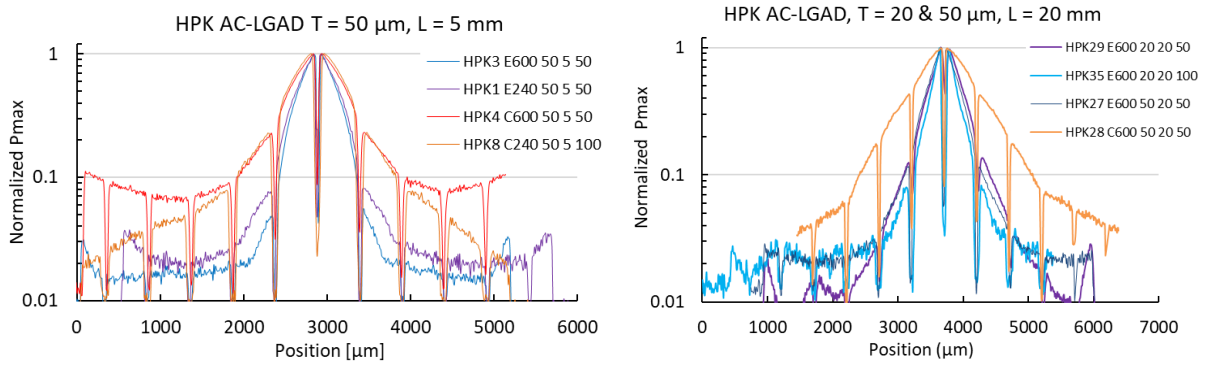


Fig. 4 Normalized Pmax distributions: LEFT of four AC-LGADs with strip length  $L = 5$  mm; RIGHT E600 and C600 type sensors with strip length  $L = 20$  mm and bulk thickness  $T = 20$  &  $50$   $\mu\text{m}$ , (Legends : ID#, Type, Bulk Thickness T, Strip Length L, Strip Width W).

The strip length influences the sharing to the next neighbor. Fig.4 RIGHT shows the Pmax distributions for sensors with 20 mm length and different bulk thicknesses. The short- and long-distance sharing to the next neighbors is worse for the E600 sensor with strip length  $L = 20$  mm than for one with  $L = 5$  mm. Yet there is little difference between E240 with strip length  $L = 5$  mm having a coupling capacitance of  $CC = 60$  pF and E600 with  $L = 20$  mm and  $CC = 600$  pF. How the sharing changes with the thickness of the bulk  $T$  is shown in Fig 4 RIGHT: a thinner E600 sensor with  $T = 20$   $\mu\text{m}$  has a better suppression of long-distance sharing than the one with  $T = 50$   $\mu\text{m}$ . In addition, the thinner detector with narrow metal width  $W = 50$   $\mu\text{m}$  has much less long-range sharing than the one with  $W = 100$   $\mu\text{m}$ . As before, the C600 sensor with  $T = 50$  shows large sharing diminishing at large distance.

### 3.3 Position Resolution

The TCT laser scans are being used to evaluate the position resolution across the strips, based on the normalized Pmax distributions between neighboring pairs of strips as shown in Fig. 5 for two AC-LGAD with 5 mm long strips, one a C240 (LEFT) and the other an E600 (RIGHT), respectively. The fraction  $Frac$  [7] is defined as

$$Frac = \frac{Pmax(1)}{[Pmax(1) + Pmax(2)]}$$

and shown as function of the position in Fig. 6 LEFT. Both the inter-strip region for Pmax and the Frac distributions are different for E and C Types. The fraction shows a close to linear behavior between deep “notches” at the location of the strip centers, and this region shown in Fig. 6 RIGHT for all 10 sensors is

used to calculate the slope  $dFrac/dPos$ . The slope of fraction vs. position is very similar separately for E and C sensors, independent of strip length, width and of the bulk thickness T. The linear slope for the C-Type sensors is a factor 1.7 smaller than for the E-Type sensors and covers a much smaller position range, which means that the position resolution needs to be calculated for a large part using the 2<sup>nd</sup> neighbor.

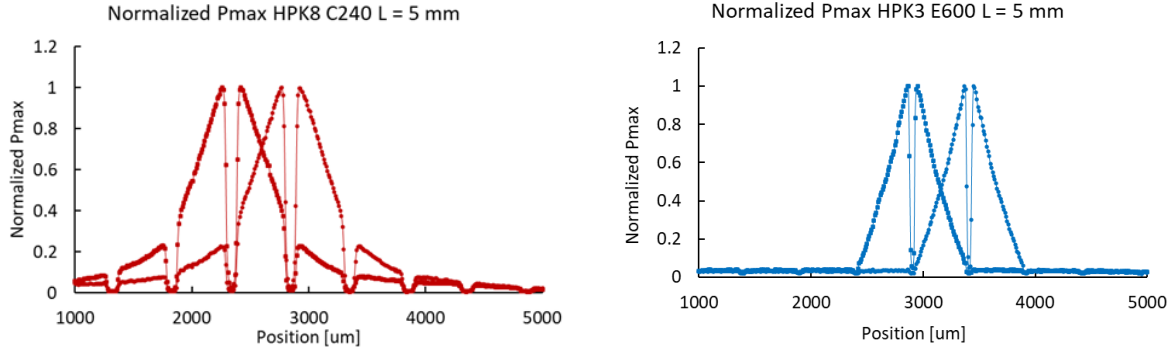


Fig. 5 Normalized Pmax distribution of two neighboring strips of LEFT C240 and RIGHT E600 sensors

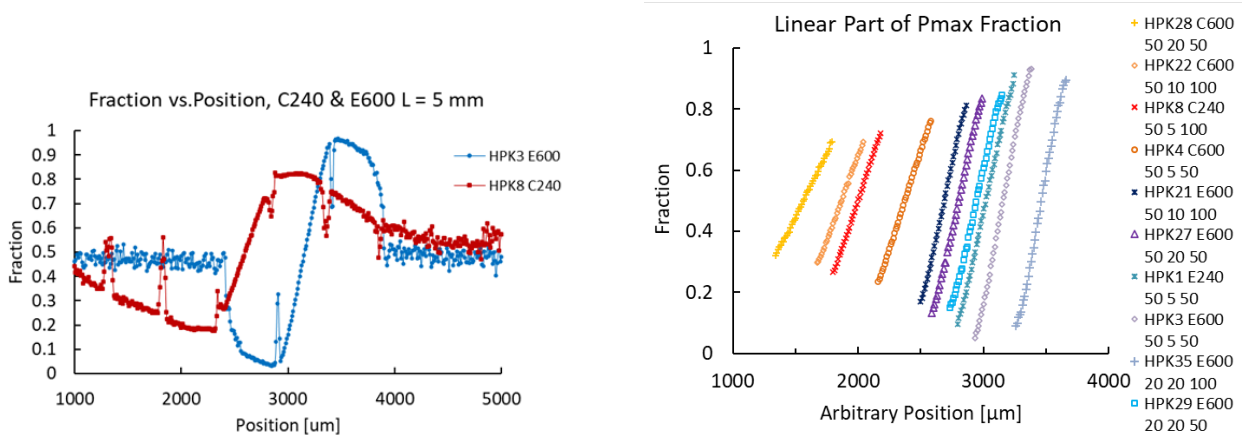


Fig. 6 Position dependence of the fraction: LEFT for the sensors of Fig. 5, RIGHT for all sensors in the region of a linear slope, with two distinct groups in slope (C-Type red/yellow, E-Type blue) (Legends : ID#, Type, Thickness T, Strip Length L, Strip Width W)

The position resolution  $\sigma(Pos)$  is calculated from the inverse of the Frac slope  $dFrac/dPos$ , i.e.  $(dPos/dFrac)$  and the signal-to-noise ratio S/N:

$$\sigma(Pos) = \sqrt{2} \left( \frac{dPos}{dFrac} \right) \frac{1}{S/N}$$

and is shown in Fig. 7 as a function of S/N. Like the fraction slope, the predicted resolution falls into two groups depending on the resistance of the N<sup>+</sup> layer, independent of the coupling capacitance. Again, the advantage of the E-Type sensors is shown by the better position resolution compared to C-Type for the same signal height. For an achievable  $S/N \geq 100$  a position resolution of  $\sigma(Pos) \leq 8 \mu m$  is reached for the E types independently of strip length, bulk thickness and metal width. There is an outlier, HPK28, which

is a 20 mm long C600 sensor shown in Fig.4 RIGHT where the excessive neighbor sharing causes an inferior position resolution, leading to a reduced Pmax as seen in Fig. 3.

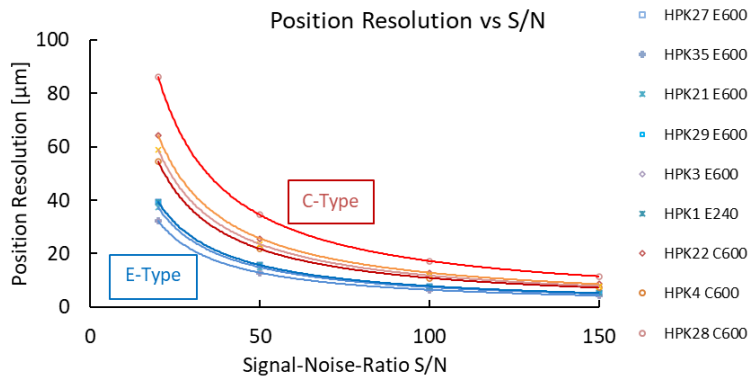


Fig. 7 Projected position resolution vs. signal-to-noise ratio S/N for the 500 um pitch sensors.

#### 4. Conclusions

In AC-LGADs, signal sharing needs to be high between neighboring strips for good position resolution and low for far-distant strips to reduce pick-up noise. Using IR laser TCT, we have investigated the sharing in HPK sensors with variations of the parameters governing the sharing, i.e. the sheet resistance of the  $N^+$  layer and the capacitance of the dielectric. Sensors with different layout of the metal strips were measured. The parameter choice “E600” gives good performance up to a strip length of 20 mm. It combines high sheet resistance of the  $N^+$  layer with large coupling capacitance (thin di-electric layer). It maximizes the pulse height of the signal, leading to lower operating bias voltage, maximizes the amount of next neighbor sharing for good position resolution and reduces the long-distance noise pick-up to the % level. A bulk thickness of 20  $\mu\text{m}$  has the lowest long-distance pick-up. Assuming a realistic signal-to-noise ratio, the high resistance E-type sensor promises an excellent position resolution of about 10  $\mu\text{m}$  on a strip pitch of 500  $\mu\text{m}$  for all tested strip parameters.

#### 5. Acknowledgements

We acknowledge the collaboration with the KEK group (K. Nakamura et al.), the FNAL group (A. Apresyan et al.) and the BNL group (A. Tricoli et al.). H.F.W.S. wants to thank the local organizing committee for the perfect organization and the very pleasant atmosphere of HSTD13.

This work was supported by the United States Department of Energy grant DE-FG02-04ER41286 and by the U.S.-Japan Science and Technology Cooperation Program in High Energy Physics.

#### 6. References

- [1] G. Pellegrini et al., Technology developments and first measurements of Low Gain Avalanche Detectors (LGAD) for high energy physics applications, NIM. A765 (2014) 12 – 16.
- [2] H. F.-W. Sadrozinski et al., Ultra-fast silicon detectors (UFSD), NIM. A730 (2013) 226–231.
- [3] H.F.-W. Sadrozinski, A. Seiden, N. Cartiglia, “4D Tracking with ultra-fast silicon detectors”, Rep. Progr. Phys. 81 (2) (2018).

- [4] M. Mandurrino et al., Demonstration of 200-, 100-, and 50- micron Pitch Resistive AC-Coupled Silicon Detectors (RSD) with 100% Fill-Factor for 4D Particle Tracking, IEEE Electron Device Letters, vol. 40, no. 11, pp. 1780-1783, Nov. 2019.
- [5] M. Tornago et al., Resistive AC-Coupled Silicon Detectors: Principles of operation and first results from a combined analysis of beam test and laser data, NIM 1003 (2021), 165319.
- [6] I. Kita et al., Development of AC-LGAD detector with finer pitch electrodes for high energy physics experiments, May 2023 arXiv:2305.12355v1.
- [7] J. Ott et al., Investigation of signal characteristics and charge sharing in AC-LGADs with laser and test beam measurements, NIM 1045 (2023), 167541.
- [8] R. Heller et al., Characterization of BNL and HPK AC-LGAD sensors with a 120 GeV proton beam, 2022 JINST 17 P05001 [arXiv:2201.07772].
- [9] Particulars, Advanced Measurement Methods, <http://particulars.si/products.php>